

Calculated elastic and thermodynamic properties of $\text{Al}_{18}\text{Mg}_3\text{M}_2$ (M = Sc, Ti, Cr, Mn and Zr) phases

DU XIAOMING^{a,*}, DONG ZHEN BIAO^a, LI JING^b, WU ERDONG^b

^a*School of Materials Science and Engineering, Shenyang Ligong University, Shenyang 110159, China*

^b*Institute of Metal Research, Chinese Academy of Sciences, Shenyang 110016, China*

Elastic and thermodynamic properties of the $\text{Al}_{18}\text{Mg}_3\text{M}_2$ (M = Sc, Ti, Cr, Mn and Zr) phases with cubic structure were investigated by means of first-principles calculations within the framework of density functional theory. The three independent single-crystal elastic constants were calculated, showing that the $\text{Al}_{18}\text{Mg}_3\text{M}_2$ phases are mechanically stable structures. Then the bulk modulus B , Young's modulus E , shear modulus G and Poisson's ratio ν were estimated for polycrystalline $\text{Al}_{18}\text{Mg}_3\text{M}_2$ from the elastic constants by the Voigt–Reuss–Hill (VRH) approximation. The ductility of $\text{Al}_{18}\text{Mg}_3\text{M}_2$ phases was analyzed, and $\text{Al}_{18}\text{Mg}_3\text{Sc}_2$ possesses the greatest plasticity or ductility. The elastic anisotropy was also further discussed in details. The Young's modulus for single crystal $\text{Al}_{18}\text{Mg}_3\text{M}_2$ was the highest in the $\langle 111 \rangle$ direction. Finally, thermodynamic properties such as the Debye temperatures, the specific heat, and melting temperature for the $\text{Al}_{18}\text{Mg}_3\text{M}_2$ phases were estimated from elastic properties.

(Received November 2, 2014; accepted January 22, 2015)

Keywords: $\text{Al}_{18}\text{Mg}_3\text{M}_2$ phases, First-principles calculations, Elastic properties, Thermodynamic properties

1. Introduction

Aluminum-magnesium (Al-Mg) alloys are good lightweight structural materials with low density (relatively high strength to weight ratio), high specific stiffness, good corrosion resistance and ductility. They have been widely used in many different fields including automotive, aerospace, marine and microelectronics industries. However, the relatively poor high-temperature mechanical properties also limits the role they play in the wider fields. Al-Mg alloys usually contain additives of transition metals, such as Mn, Cr, Sc, Ti and Zr and other metals. Small concentrations of transition metals increase the tensile strength [1,2], corrosion resistance [3] of these alloys. To further improve the performance of these alloys, a large number of experiments and theoretical explorations on microstructure, strengthening mechanism, workability and mechanical properties have been reported for Al-Mg-Sc alloys [4-9].

However relatively few researches of mechanical and thermodynamic properties of Al-Mg-M (M= Ti, Cr, Mn and Zr) alloys were implemented so far. Kerimov et al. [10,11] reported the first time the crystal structures of the ternary intermetallic Al-Mg-Transition metal (Ti, V, Cr, Mo, W, Ta) phases, which have been found to crystallize in cubic symmetry. Recently, Zhang et al. [12] reported that the elastic and electronic properties of cubic $\text{Al}_{18}\text{Ti}_2\text{Mg}_3$ phase from the first principle calculation. In our recent works, the structural, electronic properties and stability of $\text{Al}_{18}\text{Mg}_3\text{M}_2$ (M = Sc, Ti, Cr, Mn and Zr)

compounds were performed by the first-principle calculations. It was found that the addition transition metals to Al-Mg alloys has an important effect on the bonding characteristics and interaction strength between Al and transition metal atoms, Al and Mg, Al and Al [13]. However, What elastic and thermodynamic properties can be expected within the $\text{Al}_{18}\text{Mg}_3\text{M}_2$ system? How do the mechanical properties of the polycrystalline materials exhibit?

Values of the elastic constants can provide valuable information about the bonding character between adjacent atomic planes and the anisotropic character of the bonding and structural stability. It is essential to understand the actual applications of $\text{Al}_{18}\text{Mg}_3\text{M}_2$ phases. In this paper, authors attempt to calculate the elastic and thermodynamic properties of $\text{Al}_{18}\text{Mg}_3\text{M}_2$ (M= Sc, Ti, Cr, Mn and Zr) phases by first-principle calculations. Our aim is to provide reference data for experimentalists and to contribute towards a better understanding of this class of alloys.

2. Computational method

Our calculations are based on the density functional theory, using so called Quantum-ESPRESSO program package [14], in conjunction with the generalized-gradient approximations (GGA) of PW91 adopted for all elements in our models by adopting the Perdew–Burke–Ernzerhof parameters [15,16]. Ultrasoft pseudopotentials [17]

represented in reciprocal space are used. We use the following parameters for the present calculations: Conjugate gradient optimization of the wave functions, reciprocal-space integration with a Monkhorst-Pack scheme [18], energy cutoff of 500 eV, k -points grid of $6 \times 6 \times 6$. The total energies are calculated self-consistently with the tetrahedron method [19]. Electronic self-consistent field (SCF) tolerance is less than 5.0×10^{-5} eV/atom. Hellmann–Feynman force is below 0.01 eV/Å. The maximum stress is less than 0.05 GPa and displacement is within 2.0×10^{-4} Å. Convergence with respect to the k -point sampling for the Brillouin zone (BZ) integration was tested independently on the the phases using regular meshes of increasing density. Tests indicated that the total energy converges to 2 meV/atom. Pulay density mixing scheme was applied for the electron energy minimization process. The valence electronic configurations were Al ($3s^2 3p^1$), Mg ($2p^6 3s^2$), Ti ($3s^2 3p^6 3d^2 4s^2$), Cr ($3s^2 3p^6 3d^5 4s^1$), Mn ($3s^2 3p^6 3d^5 4s^2$), Sc ($3s^2 3p^6 3d^1 4s^2$), Zr ($4s^2 4p^6 4d^2 5s^2$) in the calculations.

In present work, the original crystal configurations of $\text{Al}_{18}\text{Mg}_3\text{M}_2$ ($M = \text{Sc}, \text{Ti}, \text{Cr}, \text{Mn}$ and Zr) phases in the cubic structure with the space group Fd-3m (No.227) were chosen from the X-ray diffraction results given in Ref. [11]. The unit cell has 184 atoms in which the Al atoms occupy the 48f (0.4843,0.125,0.125) and 96g (0.0584,0.0584,0.3252) Wyckoff sites, the transition metal atoms occupy 16d (0.5,0.5,0.5) sites and the Mg atoms occupy the 8a (0.125,0.125,0.125) sites and 16c (0,0, 0) sites, as shown in Fig. 1. Starting from the above crystal structure, the structural optimization was first performed by full relaxation of cell shape and atomic positions. Then the calculations of elastic and thermodynamic properties were based on the optimized equilibrium structures.

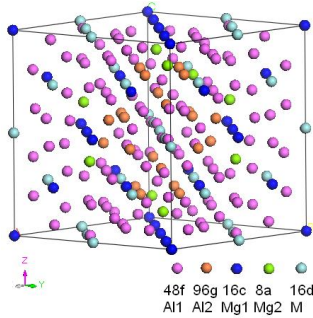


Fig. 1. Crystal structure of $\text{Al}_{18}\text{Mg}_3\text{M}_2$ ($M = \text{Sc}, \text{Ti}, \text{Cr}, \text{Mn}$ and Zr).

The elastic constants determine the stiffness of a crystal against an externally applied strain. For small deformations a linear dependence of the stress on the strain is observed (Hooke's law). Hooke's law can be generalized to account for multiaxial loading conditions as well as the elastic anisotropy. For the cubic structure such as $\text{Al}_{18}\text{Mg}_3\text{M}_2$ Phases ($M = \text{Sc}, \text{Ti}, \text{Cr}, \text{Mn}$ and Zr), the number of independent elastic constants is three (C_{11}, C_{12}

and C_{44}) and the generalized Hooke's law can be written as [20]

$$\sigma_{ij} = C_{ijkl} \varepsilon_{kl} \quad (1)$$

where σ_{ij} is the stress tensor, ε_{kl} is the Lagrangian strain tensor, and C_{ijkl} is the elastic constant tensor which is a 6×6 matrix. The symmetry present in the crystal structure may make some of these tensors equal and others may be fixed at zero. For the cubic structure, Eq. (1) can be given as follows:

$$\begin{pmatrix} \sigma_1 \\ \sigma_2 \\ \sigma_3 \\ \tau_4 \\ \tau_5 \\ \tau_6 \end{pmatrix} = \begin{pmatrix} C_{11} & C_{12} & C_{12} & 0 & 0 & 0 \\ C_{12} & C_{11} & C_{12} & 0 & 0 & 0 \\ C_{12} & C_{12} & C_{11} & 0 & 0 & 0 \\ 0 & 0 & 0 & C_{44} & 0 & 0 \\ 0 & 0 & 0 & 0 & C_{44} & 0 \\ 0 & 0 & 0 & 0 & 0 & C_{44} \end{pmatrix} \begin{pmatrix} \varepsilon_1 \\ \varepsilon_2 \\ \varepsilon_3 \\ \gamma_4 \\ \gamma_5 \\ \gamma_6 \end{pmatrix} \quad (2)$$

where C_{ij} is the elastic constant; σ_i and τ_i are the normal stress and shear stress, correspondingly, ε_i and γ_i are the normal strain and shear strain, respectively. The full elastic constants of $\text{Al}_{18}\text{Mg}_3\text{M}_2$ phases ($M = \text{Sc}, \text{Ti}, \text{Cr}, \text{Mn}$ and Zr) with cubic structure can be determined by strain pattern $(\varepsilon_1 \ 0 \ 0 \ \gamma_4 \ 0 \ 0)^T$. We substituted the strain pattern into Eq. (2), then obtained $\sigma_1 = C_{11}\varepsilon_1$, $\sigma_2 = C_{12}\varepsilon_1$ and $\tau_4 = C_{44}\gamma_4$. Finally, the three independent elastic constants (C_{11}, C_{12} and C_{44}) of $\text{Al}_{18}\text{Mg}_3\text{M}_2$ were calculated.

3. Results and discussions

3.1 Elastic constants and mechanical stability

Elastic constants are the measure of the resistance of a crystal to an externally applied stress. Through imposing small strain on the perfect lattice, the elastic constants can be obtained. The values of elastic stiffness constants (C_{11}, C_{12} and C_{44}) and elastic compliance constants (S_{11}, S_{12} and S_{44}) for $\text{Al}_{18}\text{Mg}_3\text{M}_2$ phases ($M = \text{Sc}, \text{Ti}, \text{Cr}, \text{Mn}$ and Zr) were presented in Table 1, along with the available experimental data and previously calculated values obtained by ab initio techniques. The addition of Mg and transition metal atoms to Al matrix can influence particular elastic constants in different way. Comparing with pure aluminum and $\text{Al}_{12}\text{Mg}_{17}$, elastic constants C_{11} and C_{44} increase for $\text{Al}_{18}\text{Mg}_3\text{M}_2$ ($M = \text{Ti}, \text{Cr}, \text{Mn}$ and Zr) phases, whereas decreases for $\text{Al}_{18}\text{Mg}_3\text{Sc}_2$ phase. It is indicated that normal stresses in three crystal direction (σ_1, σ_2 and σ_3) and shear stresses (τ_4, τ_5 and τ_6) increase (or decreases) for $\text{Al}_{18}\text{Mg}_3\text{M}_2$ ($M = \text{Ti}, \text{Cr}, \text{Mn}$ and Zr) phases (or $\text{Al}_{18}\text{Mg}_3\text{Sc}_2$). However, elastic constant C_{12} does not show clear tendency. Moreover, the elastic constants of $\text{Al}_{18}\text{Mg}_3\text{Ti}_2$ phase here are good agreement with the calculated results in Ref. [12] (see Table 1). To our knowledge, there have been no experimental and

theoretical values of the elastic constants on $\text{Al}_{18}\text{Mg}_3\text{M}_2$ ($M = \text{Sc}, \text{Cr}, \text{Mn}$ and Zr) phases.

The intrinsic mechanical stability of a solid is in general determined by certain conditions related to the crystal symmetry. For cubic lattice, the criteria of

mechanical stability is that C_{44} , $C_{11}-C_{12}$ and $C_{11}+2C_{12}$ must be positive. The calculated results of $\text{Al}_{18}\text{Mg}_3\text{M}_2$ ($M = \text{Sc}, \text{Ti}, \text{Cr}, \text{Mn}$ and Zr) phases obey all of the above criteria, and indicate that the phases are mechanically stable.

Table 1. The calculated elastic constants, C_{ij} (in GPa) and S_{ij} (1/GPa) for $\text{Al}_{18}\text{Mg}_3\text{M}_2$ phases ($M = \text{Sc}, \text{Ti}, \text{Cr}, \text{Mn}$ and Zr).

Species	C_{11}	C_{12}	C_{44}	S_{11}	S_{12}	S_{44}
$\text{Al}_{18}\text{Mg}_3\text{Sc}_2$	101.6	48.1	24.7	0.014	-0.0045	0.041
$\text{Al}_{18}\text{Mg}_3\text{Ti}_2$	131.7	52.8	47.9	0.0099	-0.0028	0.021
$\text{Al}_{18}\text{Mg}_3\text{Ti}_2^a$	131	50	56	-	-	-
$\text{Al}_{18}\text{Mg}_3\text{Cr}_2$	145.5	56.8	55.0	0.0088	-0.0025	0.018
$\text{Al}_{18}\text{Mg}_3\text{Mn}_2$	144.5	62.0	49.3	0.0093	-0.0028	0.020
$\text{Al}_{18}\text{Mg}_3\text{Zr}_2$	114.8	49.3	48.0	0.011	-0.0035	0.021
Pure Al ^b	114.3	61.9	31.6	-	-	-
$\text{Al}_{12}\text{Mg}_{17}^c$	97.7	28.1	31.4	-	-	-

^a Ref. [12], ^b Ref. [21], ^c Ref. [22].

3.2 Elastic properties for polycrystalline aggregates

To account for a polycrystalline material, the upper and lower bounds (Reuss [23] and Voigt [24]) of bulk (B_R , B_V) and shear (G_R , G_V) modulus are found from single crystal elastic constants. Voigt assumes that the strain in the polycrystalline aggregate to the external strain is uniform, while Reuss assumes the stress in the polycrystalline aggregate to the external stress is uniform. The Voigt shear modulus G_V and the Reuss shear modulus G_R for cubic lattices are:

$$G_V = (C_{11} - C_{12} + 3C_{44}) / 5 \quad (3)$$

and

$$G_R = 5 / (4S_{11} - 4S_{12} + 3S_{44}) \quad (4)$$

respectively, and the Voigt bulk modulus B_V and the Reuss bulk modulus B_R are defined as:

$$B_V = (C_{11} + 2C_{12}) / 3 \quad (5)$$

and

$$B_R = 1 / (3S_{11} + 6S_{12}) \quad (6)$$

respectively. In Eqs. (4) and (6), S_{ij} is the elastic compliance constants. Subsequently, a simple average of those bound values of B_R , B_V and G_R , G_V was calculated as proposed by Hill [25]. The bulk modulus and shear modulus are:

$$B_H = (B_V + B_R) / 2 \quad (7)$$

and

$$G_H = (G_V + G_R) / 2 \quad (8)$$

respectively. Additionally the Young modulus E_H and Poisson ratio ν_H have been calculated using Hill's empirical average and the equations:

$$E_H = 9B_H G_H / (3B_H + G_H) \quad (9)$$

and

$$\nu_H = (3B_H - 2G_H) / (6B_H + 2G_H) \quad (10)$$

All calculated results based on Eqs. (3)-(10) are listed in Table 2. Note that the difference between B_V and B_R as well as between G_V and G_R is comparatively small. As seen from Table 2, the calculated bulk modulus of $\text{Al}_{18}\text{Mg}_3\text{Mn}_2$ is highest, indicating that the resistance to volume change by applied pressure is eventually improved. The shear modulus and Young's modulus of $\text{Al}_{18}\text{Mg}_3\text{Cr}_2$ are highest. And G_H , B_H and E_H of $\text{Al}_{18}\text{Mg}_3\text{Sc}_2$ are smallest.

The ratio of the bulk modulus to shear modulus of crystalline phases, proposed by Pugh [26], can empirically predict the brittle and ductile behavior of materials. A high B/G ratio is associated with ductility, whereas a low value corresponds to brittle nature. The critical value which separates ductile and brittle material is around 1.75. The calculated results in Table 2 show that $\text{Al}_{18}\text{Mg}_3\text{Ti}_2$, $\text{Al}_{18}\text{Mg}_3\text{Sc}_2$ and $\text{Al}_{18}\text{Mg}_3\text{Mn}_2$ phases exhibit good ductility. Whileas $\text{Al}_{18}\text{Mg}_3\text{Cr}_2$ and $\text{Al}_{18}\text{Mg}_3\text{Zr}_2$ are brittle. Besides B/G , it is found that $C_{11}-C_{12}$ and Young's modulus E are another two significant indications of the mechanical properties of materials [27]. The smaller the values of $C_{11}-C_{12}$ and Young's modulus are, the better the plasticity is. From the results in Tables 1 and 2, it can be seen that $\text{Al}_{18}\text{Mg}_3\text{Sc}_2$ has lowest values of $C_{11}-C_{12}$ and Young's modulus E , implying the greatest plasticity. On the other hand, Poisson's ratio ν_H is used to quantify the stability of the crystal against shear, which usually ranges from -1 to 0.5. The larger the Poisson's ratio is, the better the

plasticity is. In Table 2, it can be seen that $Al_{18}Mg_3Sc_2$ has a greatest Poisson's ratio equal to 0.329, showing that it has also a greatest plasticity compared to the rest. Whereas $Al_{18}Mg_3Cr_2$ has a poorest plasticity with Poisson's ratio equal to 0.255. Therefore, addition of Sc to Al-Mg based alloys could effectively improve the ductility (or plasticity). Considering the lower stiffness and the cubic structure, $Al_{18}Mg_3Sc_2$ phase might be easy to deform than other four phases under outer stress. Very fine-grained Al-Mg-Sc alloys have been tested to tensile elongation values

of 1000% [28,29], and many results have been published on high strain-rate superplasticity of Al-Mg-Sc alloys with fine grains produced by equalangular channel pressing (ECAP) [30,31]. The addition of Cr to Al-Mg based alloys however makes materials brittle. The rigidity of $Al_{18}Mg_3Cr_2$ is also improved due to the highest Young's modulus, E_H (Table 2).

Table 2. The calculated values of shear modulu (in GPa), G_V , G_R and G_H , bulk modulu (in GPa), B_V , B_R and B_H , Young's modulus (in GPa), E_H , Poisson's ratio, ν_H and B/G of $Al_{18}Mg_3M_2$ ($M = Sc, Ti, Cr, Mn$ and Zr) phases.

	$Al_{18}Mg_3Sc_2$	$Al_{18}Mg_3Ti_2$	$Al_{18}Mg_3Cr_2$	$Al_{18}Mg_3Mn_2$	$Al_{18}Mg_3Zr_2$
G_R	25.5	44.1	50.3	45.7	40.5
G_V	25.5	44.5	50.7	46.1	41.9
G_H	25.5	44.3	50.5	45.9	41.2
B_R	65.9	79.1	86.3	89.5	71.2
B_V	65.9	79.1	86.3	89.5	71.2
B_H	65.9	79.1	86.3	89.5	71.2
E_H	67.8	112	127	118	104
ν_H	0.329	0.264	0.255	0.281	0.257
B/G	2.58	1.79	1.71	1.95	1.73

3.3 Elastic anisotropy

The elastic constants of solids are very important because they are closely associated with the mechanical and physical properties. In particular, they play an important part in providing valuable information about structural stability and anisotropic characteristics. In present work, we calculated two anisotropic indexes of single crystal proposed by Zener [32] and Every [33], which are listed as follows, respectively:

$$A_Z = 2C_{44} / (C_{11} - C_{12}) \quad (11)$$

$$A_E = (C_{11} - C_{12} - 2C_{44}) / (C_{11} - C_{44}) \quad (12)$$

For an isotropic crystal the standard values of A_Z and A_E must be 1 and 0, respectively. Obviously, the small deviations of the two indexes from A_Z and A_E imply elastic

isotropy of materials. The calculated values listed in Table 3 show that all $Al_{18}Mg_3M_2$ phases are anisotropic.

The elastic anisotropy in compressibility and shear was also investigated using two dimensionless quantities $A_B = (B_V - B_R) / (B_V + B_R)$ and $A_G = (G_V - G_R) / (G_V + G_R)$, respectively [34]. The subscripts V and R designate the Voigt and Reuss bounds, which represent the maximum and minimum limits of the polycrystalline elastic modulus. The value of zero represents elastic isotropy and the value of unity indicates the largest possible anisotropy. The calculated values of A_B and A_G are 0 and below 2 %, respectively for all phases. Therefore, $Al_{18}Mg_3M_2$ phases do not have anisotropy in compression and exhibited small anisotropy in shear.

Table 3. The calculated anisotropic factors of $Al_{18}Mg_3M_2$ ($M = Sc, Ti, Cr, Mn$ and Zr) phases.

Species	A_Z	A_E	A_B	A_G
$Al_{18}Mg_3Sc_2$	0.92	0.053	0	0
$Al_{18}Mg_3Ti_2$	1.21	-0.20	0	0.0045
$Al_{18}Mg_3Cr_2$	1.24	-0.24	0	0.0040
$Al_{18}Mg_3Mn_2$	1.20	-0.17	0	0.0044
$Al_{18}Mg_3Zr_2$	1.47	-0.46	0	0.017

The orientation dependence of the Young's modulus on a single crystal can be obtained from the elastic compliance coefficients S_{ij} . For the case of the cubic system, it can be shown that the Young's modulus in any

given direction is given in terms of the three independent elastic compliance coefficients and the direction cosines of the crystallographic direction [35]:

$$\frac{1}{E} = S_{11} - 2(S_{11} - S_{12} - \frac{1}{2}S_{44})(l_1^2 l_2^2 + l_1^2 l_3^2 + l_2^2 l_3^2) \quad (13)$$

where l_1 , l_2 , and l_3 are the directional cosines, and they can be obtained by $l_1 = \sin[\theta]\cos[\varphi]$, $l_2 = \sin[\theta]\sin[\varphi]$ and $l_3 = \cos[\theta]$ in spherical coordinates. The angles θ and φ are well defined in spherical coordinates. S_{ij} is defined as an elastic compliance matrix (i.e., the inverse of the elastic stiffness matrix) (see Table 1). Considering the $Al_{18}Mg_3M_2$ series studied here exhibit similar features, accordingly we have only documented such plots for $Al_{18}Mg_3Sc_2$ phase. Fig. 2 shows the orientation dependence of the Young's modulus for $Al_{18}Mg_3Sc_2$ phase. For an isotropic system, the orientation dependence of Young's modulus should be spherical shape. As can be

seen from Fig. 2 (a), the Young's modulus graph for $Al_{18}Mg_3Sc_2$ phase exhibits ellipsoidal shape which indicates that the Young's modulus of the phase is anisotropic. This agrees with the analyses of elastic anisotropic indexes (Table 3). Fig. 2 (b)-(d) give the distribution shape of the Young's modulus in different crystal planes, clearly showing the anisotropy in the x-z (a-c) and y-z (b-c) planes. The Young's modulus along special crystal directions are summarized in Table 4 for all phases. The value of the Young's modulus for the $\langle 111 \rangle$ direction is the highest of all directions and about two times as large as that for the $\langle 100 \rangle$ direction, except for $Al_{18}Mg_3Sc_2$ phase. This means that single crystal $Al_{18}Mg_3M_2$ phases exhibit a large elastic anisotropy.

Table 4. The Young's modulus of $Al_{18}Mg_3M_2$ ($M = Sc, Ti, Cr, Mn$ and Zr) phases along special crystal directions (in GPa).

Species	$\langle 100 \rangle$	$\langle 010 \rangle$	$\langle 001 \rangle$	$\langle 110 \rangle$	$\langle 111 \rangle$
$Al_{18}Mg_3Sc_2$	71.4	71.4	71.4	62.5	56.1
$Al_{18}Mg_3Ti_2$	101	101	101	130	176
$Al_{18}Mg_3Cr_2$	114	114	114	154	227
$Al_{18}Mg_3Mn_2$	108	108	108	139	189
$Al_{18}Mg_3Zr_2$	90.9	90.9	90.9	143	299

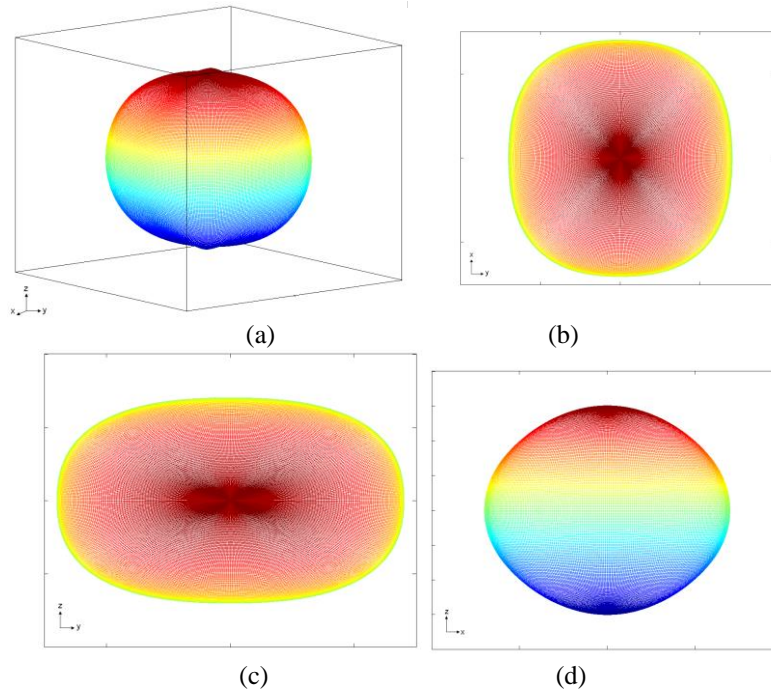


Fig. 2. Directional dependence of Young's modulus for $Al_{18}Mg_3Sc_2$, (a) three-dimensional surfaces, the projections of Young's modulus at (b) x-y plane; (c) y-z plane; (d) x-z plane.

3.4 Thermodynamic properties

The Debye temperature θ_D is a fundamental attribute of a solid connecting elastic properties with thermodynamic properties such as specific heat, sound velocity and melting temperature. It can be calculated

from the averaged sound velocity, v_m by the following equation [36]:

$$\theta_D = \frac{h}{k_B} \left[\frac{3n}{4\pi} \left(\frac{N_A \rho}{M} \right) \right]^{\frac{1}{3}} v_m \quad (14)$$

where h is Planck's constant, k_B is Boltzmann's constant, N_A is Avogadro's number, n is the number of atoms in the

unit cell, M is the molecular weight and ρ is the density. The average sound velocity in the polycrystalline material is approximately given by [36]:

$$v_m = \left[\frac{1}{3} \left(\frac{2}{v_s} + \frac{1}{v_l} \right) \right]^{-1/3} \quad (15)$$

where v_l and v_s are the longitudinal and transverse sound velocity, respectively, which can be obtained using the shear modulus G and the bulk modulus B from Navier's equations [37]:

$$v_l = \sqrt{\frac{B + 4G/3}{\rho}} \quad \text{and} \quad v_s = \sqrt{\frac{G}{\rho}} \quad (16)$$

The calculated sound velocity and Debye temperature as well as the density for the $\text{Al}_{18}\text{Mg}_3\text{M}_2$ phases are given in Table 5. The Debye temperature of $\text{Al}_{18}\text{Mg}_3\text{M}_2$ phases increases from Sc to Cr, however, it decreases from Mn to Zr. That is, $\text{Al}_{18}\text{Mg}_3\text{Cr}_2$ has the highest Debye temperature, suggesting that $\text{Al}_{18}\text{Mg}_3\text{Cr}_2$ is hardest. The Debye temperature is lowest for $\text{Al}_{18}\text{Mg}_3\text{Sc}_2$,

suggesting that $\text{Al}_{18}\text{Mg}_3\text{Sc}_2$ is softest. Unfortunately, as far as we know, there are no experimental data available related to these properties in the literature for the $\text{Al}_{18}\text{Mg}_3\text{M}_2$ phases which are studied here.

In the approximation of Debye model, the specific heat of the solid, C_v can be obtained from Debye temperature by the following equation [38]

$$C_v = 9N_A k_B (T/\theta_D)^3 \int_0^{\theta_D/T} \frac{x^4 e^x}{(e^x - 1)^2} dx \quad (17)$$

where T is the temperature (K). The calculated values of the specific heat of the $\text{Al}_{18}\text{Mg}_3\text{M}_2$ phases are shown in Fig. 3. The specific heat of the $\text{Al}_{18}\text{Mg}_3\text{M}_2$ phases is similar and increases with increasing temperature below θ_D . However, the specific heat of these phases is gradually close to 25 J/mol·K for the high temperature case ($T \gg \theta_D$), which is the Dulong-Petit result (equal to $3N_A k_B$) from classical thermodynamics. For low temperature case ($T \ll \theta_D$), the electron specific heat becomes significant for metals and is combined with the above specific heat in the Einstein-Debye specific heat [39].

Table 5. The calculated density (ρ), the longitudinal, transverse, and average sound velocity (v_l , v_s , v_m), the Debye temperatures (θ_D) and the melting temperature (T_m).

Phase	v_l ($\text{m}\cdot\text{s}^{-1}$)	v_s ($\text{m}\cdot\text{s}^{-1}$)	v_m ($\text{m}\cdot\text{s}^{-1}$)	ρ ($\text{kg}\cdot\text{m}^{-3}$)	θ_D (K)	T_m (K)
$\text{Al}_{18}\text{Mg}_3\text{Sc}_2$	2010	1015	1138	2524	804	853
$\text{Al}_{18}\text{Mg}_3\text{Ti}_2$	2363	1338	1488	2678	1068	1031
$\text{Al}_{18}\text{Mg}_3\text{Cr}_2$	2492	1429	1587	2875	1167	1113
$\text{Al}_{18}\text{Mg}_3\text{Mn}_2$	2468	1362	1517	2939	1111	1107
$\text{Al}_{18}\text{Mg}_3\text{Zr}_2$	2258	1291	1434	2854	1009	931

For cubic structural metals, the melting temperature, T_m can be estimated from the elastic constants. The relationship between the elastic constants and melting temperature, T_m is linear by the following empirical equation [40]:

$$T_m = 553 + (591\text{K} / \text{Mbar})C_{11} \pm 300\text{K} \quad (18)$$

In present work, a minus sign can be selected in the Eq. (18). The calculated values of the melting temperature for $\text{Al}_{18}\text{Mg}_3\text{M}_2$ phases are listed in Table 5. As seen in Table 5, the melting temperature of $\text{Al}_{18}\text{Mg}_3\text{Sc}_2$ phase is close to Al-Mg alloys. Whereas for other four $\text{Al}_{18}\text{Mg}_3\text{M}_2$ phases, the melting temperature is much higher than that of Al-Mg alloys. It can be understood due to higher Young's modulus, shear modulus and Debye temperatures for those phases.

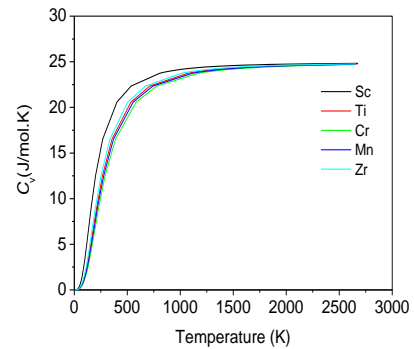


Fig. 3. The dependence of specific heat on temperature for $\text{Al}_{18}\text{Mg}_3\text{M}_2$ phases.

4. Conclusions

In summary, we have calculated and analyzed the elastic properties of the $\text{Al}_{18}\text{Mg}_3\text{M}_2$ ($M = \text{Sc, Ti, Cr, Mn}$ and Zr) phases by the plane-wave ultrasoft pseudopotential method based on the density-functional theory. We have also calculated the shear modulus, G ; Young's modulus,

E ; and Poisson's ratio for ideal polycrystalline $\text{Al}_{18}\text{Mg}_3\text{M}_2$ aggregates within the scheme of Voigt–Reuss–Hill (VRH) approximation, and the ductility was then analyzed. The elastic anisotropy was also discussed in details. The results show that $\text{Al}_{18}\text{Mg}_3\text{M}_2$ phase are mechanically stable structures. $\text{Al}_{18}\text{Mg}_3\text{Sc}_2$ possesses the best plasticity or ductility. And $\text{Al}_{18}\text{Mg}_3\text{Cr}_2$ possesses the highest rigidity due to highest Young's modulus. The calculated results of the anisotropic indexes of single crystal show that all $\text{Al}_{18}\text{Mg}_3\text{M}_2$ phases are anisotropic. The directional Young's modulus of $\text{Al}_{18}\text{Mg}_3\text{M}_2$ phases indicates that Young's modulus for the $\langle 111 \rangle$ direction is the highest in all direction. Finally, we have derived thermodynamic properties such as the sound velocity, the Debye temperatures, the specific heat, and melting temperature for the $\text{Al}_{18}\text{Mg}_3\text{M}_2$ phases.

Acknowledgement

The authors gratefully acknowledge the financial support by the program for Shenyang Ligong University Key Course Opening Fund in Materials Processing Engineering, China and by the program for Liaoning Excellent Talents in University (LNET), China (LJQ2012016).

References

- [1] V. I. Elagin, V. V. Zakharov, T. D. Rostova, *Met. Sci. Heat Treat.*, **34**, 37 (1992).
- [2] S. Lathabai, P. G. Lloyd, *Acta Mater.*, **50**, 4275 (2002).
- [3] M. N. Ishaq, S. T. A. Shah, S. Ali, *Coden, Coden Jnsmac*, **46**, 39 (2006).
- [4] L. S. Toporova, D. G. Eskin, M. L. Kharakterova, T. B. Dobatkina, *Advanced Aluminum Alloys Containing Scandium*, Amsterdam, Gordon & Breach, 1998.
- [5] R. R. Sawtell, C. L. Jensen, *Metall. Trans.*, **A21**, 421 (1990).
- [6] O. Roder, O. Schauerer, G. Lutjering, A. Gysler, *Mater. Sci. Forum*, **217-222**, 1835 (1996).
- [7] A. Gholinia, F. J. Humphreys, P. B. Prangnell, *Acta Mater.*, **50**, 4461 (2002).
- [8] O. Sitdikov, T. Sakai, E. Avtokratova, R. Kaibyshev, K. Tsuzaki, Y. Watanabe, *Acta Mater.*, **56**, 821 (2008).
- [9] Y. Miura, T. Shioyama, D. Hara, *Mater. Sci. Forum*, **217-222**, 505 (1996).
- [10] K. M. Kerimov, S. F. Dunaev, E. M. J. Sljusarenko, *J. Less-Common Met.*, **133**, 297 (1987).
- [11] K. M. Kerimov, S. F. Dunaev, *J. Less-Common Met.*, **153**, 267 (1989).
- [12] F. Y. Zhang, M. F. Yan, Y. You, C. S. Zhang, H. T. Chen, *Physica B*, **408**, 68 (2013).
- [13] X. M. Du, P. Ma, E. D. Wu, *Optoelectron. Adv. Mater. – Rapid Comm.* **8**, 916 (2014).
- [14] <http://www.pwscf.org>.
- [15] B. Hammer, L. B. Hansen, J. K. Norkov, *Phys. Rev. B*, **59**, 7413 (1999).
- [16] J. A. White, D. M. Bird, *Phys. Rev. B*, **50**, 4954 (1994).
- [17] D. Vanderbilt, *Phys. Rev. B*, **41**, 7892 (1990).
- [18] H. J. Monksorst, J. D. Pack, *Phys. Rev. B*, **13**, 5188 (1976).
- [19] P. E. Blochl, O. Jepsen, O. K. Andersen, *Phys. Rev. B*, **49**, 16223 (1994).
- [20] J. F. Nye, *Physical Properties of Crystals: Their Representation by Tensors and Matrices*, Oxford, Oxford University Press, 1985.
- [21] G. Simmons, H. Wang, *Single Crystal Elastic Constants and Calculated Aggregate Properties: A Handbook*, Cambridge, M. I. T. Press, 1971.
- [22] H. Zhang, S. L. Shang, Y. Wang, A. Saengdeejing, L. Q. Chen, Z. K. Liu, *Acta Mater.*, **58**, 4012 (2010).
- [23] A. Reuss, **9**, 49 (1929).
- [24] W. Voigt, *Lehrbuch der Kristallphysik*, 313-315, 1928, Leipzig, Taubner.
- [25] R. Hill, *Proc. Phys. Soc., London, Sect. A*, **65**, 350 (1952).
- [26] S. F. Pugh, *Phil. Mag.*, **45**, 823 (1954).
- [27] A. Sumer, J. F. Smith, *J. Appl. Phys.*, **33**, 2283 (1962).
- [28] R. R. Sawtell C. L. Jensen, *Metall. Trans. A*, **21**, 421 (1990).
- [29] T. G. Nieh, L. M. Hsiung, J. Wadsworth, R. Kaibyshev, *Acta Mater.*, **46**, 2789 (1998).
- [30] S. Komura, P. B. Berbon, M. Furukawa, Z. Horita, M. Nemoto, T. G. Langdon, *Scripta Mater.*, **38**, 1851 (1998).
- [31] H. Akamatsu, T. Fujinami, Z. Horita, T. G. Langdon, *Scripta Mater.*, **44**, 759 (2001).
- [32] C. Zener, *Elasticity and Anelasticity of Metals*, Chicago, The University of Chicago, 1948.
- [33] A. G. Every, *Phys. Rev. B*, **22**, 1746 (1980).
- [34] D. H. Chung, W. R. Buessem, *Anisotropy in single crystal refractory compounds*, in 'The Elastic Anisotropy of Crystals 2', (ed. F. W. Vahldiek, S. A. Mersol), 217-245, New York, Plenum, 1968.
- [35] J. F. Nye, *Effect of crystal symmetry on crystal properties*, in *Physical Properties of Crystals*, 2nd ed., 20-24, Oxford, UK, Clarendon Press, 1964.
- [36] O. L. Anderson, *J. Phys. Chem. Solids*, **24**, 909 (1963).
- [37] E. Schreiber, O. L. Anderson, N. Soga, *Elastic constants and their measurements*, New York, McGraw-Hill, 1973.
- [38] M. A. Blanco, E. Francisco, V. Luana, *Comput. Phys. Commun.*, **158**, 57 (2004).
- [39] <http://hyperphysics.phy-astr.gsu.edu/Hbase/Solids/phonon.html>.
- [40] M. J. Mehl, J. E. Osburn, D. A. Papaconstantopoulos, B. M. Klein, *Phys. Rev. B*, **41**, 10311 (1990).